

Figure 12: Simulated normalized power density along the transverse direction at  $R_o = 310$  mm for the FF-focused transmitarray, NF-focused transmitarray, and dual-focused transmitarray from the antenna aperture (a)  $x = 0$ . (b)  $y = 0$ .

#### 4. Design of NF/ NF and FF/FF dual- focused transmitarray

The previous concept is applied to obtain dual-focused in the near field region or dual-direction beams in the far field region. The design depends on the chess-board unit-cell element arrangement. The arrangement of the cells depends on the arrangement of the cells at different two distances in the Fresnel zone at  $R_o = 310$  mm and  $R_o = 347$  mm from the antenna aperture. Table 3 shows the phase distributions and corresponding hole radii for first quadrant of the NF/NF-Dual-focused transmitarray. The contour plot of the normalized power density in the x-y plane for the NF/NF-dual-focused transmitarray is shown in Fig.13. The contours of the power density for  $R_{o1} = 310$  mm with -10 dB spot area of  $48 \text{ mm} \times 45 \text{ mm}$  are shown in Fig.13a. The contours of the power density for  $R_{o2} = 347$  mm with -10 dB spot area of  $57 \text{ mm} \times 50 \text{ mm}$  are shown in Fig.13b. Design for FF/FF dual-focused transmitarray depends on rearranged for the cells in the array to get two beams at different angles ( $\theta = 20^\circ$  and  $\theta = -20^\circ$ ) using single structure. The chess-board design for FF/FF dual-focused transmitarray is the same as previous

one except takes cell at  $\theta = 20^\circ$  and the follow cell at  $\theta = -20^\circ$  and then interchange the sequence to start with  $\theta = -20^\circ$ . Table 4 shows the phase distributions and corresponding hole radii for first half of the dual-direction beams transmitarray. The gain for  $\theta = 20^\circ$  is 15 dB and for  $\theta = -20^\circ$  is 17 dB. The 3D power pattern of dual beam transmitarray in the same structure is shown in Fig. 14. The HPBW is  $8.6^\circ$  and  $8.5^\circ$  for  $\theta = 20^\circ$  and  $\theta = -20^\circ$ , respectively.

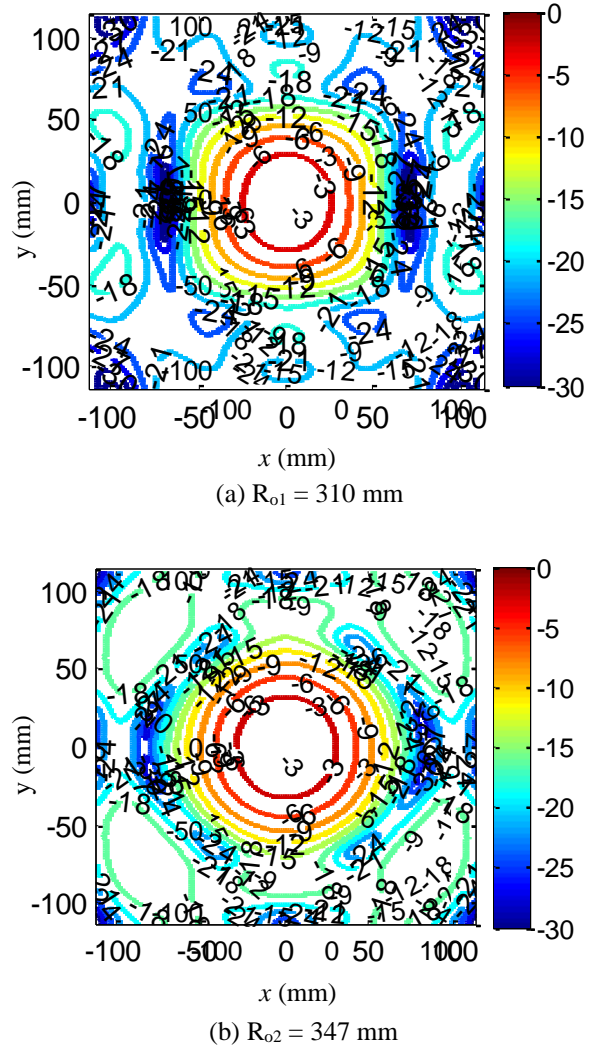


Figure 13: A contour plot of the simulated normalized power density of for the dual-focused transmitarray in a plane at (a)  $R_{o1} = 310$  mm and (b)  $R_{o2} = 347$  mm.

Table 2: The phase shift and the corresponding hole radius for FF/NF transmitarray (first quadrant).

306.00° 3.64 mm	313.67° 3.66 mm	353.92° 3.74 mm	14.12° 1.17 mm	134.71° 2.62 mm	130.24° 2.58 mm	360.38° 0.26 mm
313.67° 3.66 mm	330.02° 3.72 mm	344.11° 3.74 mm	64.86° 2.05 mm	72.94° 2.12 mm	248.86° 3.43 mm	213.61° 3.29 mm
353.92° 3.74 mm	344.11° 3.74 mm	41.34° 1.79 mm	43.73° 1.82 mm	180.70° 3.06 mm	158.36° 2.85 mm	404.29° 1.83 mm
14.12° 1.17 mm	64.86° 2.05 mm	43.73° 1.82 mm	157.76° 2.84 mm	130.24° 2.58 mm	338.27° 3.74 mm	267.59° 3.50 mm
134.71° 2.62 mm	72.94° 2.12 mm	180.70° 3.06 mm	130.24° 2.58 mm	316.07° 3.67 mm	240.75° 3.40 mm	533.81° 3.00 mm
130.24° 2.58 mm	248.86° 3.43 mm	158.36° 2.85 mm	338.27° 3.74 mm	240.75° 3.40 mm	512.45° 2.79 mm	12.12° 1.10 mm
360.38° 0.26 mm	213.61° 3.29 mm	404.29° 1.83 mm	267.59° 3.50 mm	533.81° 3.00 mm	12.12° 1.10 mm	382.88° 1.42 m

Table 3: The phase shift and the corresponding hole radius for NF/NF transmitarray (first quadrant).

306° 3.64 mm	317.56° 3 mm	353.92° 3.74 mm	48.99° 1.94 mm	134.71° 2.62 mm	226.4° 3.39 mm	360.38° 0.26 mm
317.56° 3.68 mm	330.02° 3.72 mm	363.52° 0.69 mm	64.86° 2.05 mm	138.56° 2.73 mm	248.86° 3.43 mm	355.15° 1.06 mm
353.92° 3.74 mm	363.52° 0.69 mm	41.34° 1.79 mm	94° 2.34 mm	180.7° 3.06 mm	269.7° 3.56 mm	404.29° 1.83 mm
48.99° 1.94 mm	64.86° 2.05 mm	94° 2.34 mm	157.76° 2.84 mm	226.4° 3.39 mm	338.27° 3.74 mm	439.13° 2.33 mm
134.71° 2.62 mm	138.56° 2.73 mm	180.7° 3.06 mm	226.4° 3.39 mm	316.07° 3.67 mm	397.32° 1.96 mm	533.81° 3.00 mm
226.4° 3.39 mm	248.86° 3.43 mm	269.7° 3.56 mm	338.27° 3.74 mm	397.32° 1.96 mm	512.45° 2.79 mm	243.03° 3.51 mm
360.38° 0.26 mm	355.15° 1.06 mm	404.29° 1.83 mm	439.13° 2.33 mm	533.81° 3 mm	243.03° 3.51 mm	382.88° 1.42 mm

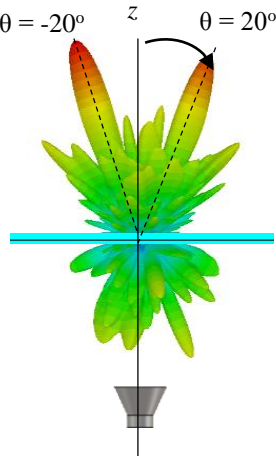


Figure 14: The 3D power pattern of dual beam transmitarray in the same structure.

Table 4: The phase shift and the corresponding hole radius for dual beam transmitarray (first half).

216.16° 3.3 mm	204.23° 3.24 mm	243.38° 3.41 mm	258.22° 3.47 mm	323.25° 3.7 mm	2.74° 0.44 mm	90.92° 2.27 mm
182.43° 3.08 mm	85.13° 2.23 mm	210.55° 3.28 mm	140.87° 2.67 mm	292.94° 3.59 mm	248.56° 3.43 mm	64.3° 2.05 mm
311.93° 3.66 mm	186.69° 3.12 mm	340.86° 3.74 mm	243.99° 3.41 mm	65.49° 2.06 mm	354.5° 3.74 mm	200.13° 3.22 mm
189.44° 3.15 mm	206.26° 3.2 mm	219.04° 3.32 mm	264.88° 3.49 mm	305.56° 3.64 mm	17.74° 1.27 mm	82.91° 2.21 mm
99.67° 2.34 mm	220.99° 3.32 mm	129.79° 2.58 mm	280.61° 3.55 mm	217.73° 3.31 mm	35.24° 1.7 mm	357.13° 3.74 mm
252.11° 3.45 mm	22.89° 1.42 mm	282.55° 3.56 mm	83.13° 2.22 mm	11.38° 1.06 mm	198.87° 3.21 mm	152.05° 2.79 mm
306° 3.64 mm	313.68° 3.66 mm	336.55° 3.74 mm	14.13° 1.17 mm	65.68° 2.06 mm	130.25° 2.58 mm	206.78° 3.26 mm
15.24° 1.21 mm	259.77° 3.47 mm	45.68° 1.85 mm	320° 3.69 mm	134.51° 2.62 mm	75.75° 2.15 mm	275.18° 3.53 mm
213.42° 3.29 mm	107.24° 2.4 mm	243.54° 3.41 mm	166.86° 2.39 mm	331.48° 3.72 mm	281.49° 3.55 mm	110.87° 2.42 mm
198.82° 3.21 mm	196.88° 3.2 mm	228.42° 3.36 mm	255.49° 3.46 mm	314.94° 3.67 mm	8.36° 0.89 mm	92.29° 2.29 mm
179.42° 3.06 mm	219.19° 3.68 mm	208.35° 3.27 mm	16.5° 1.24 mm	292.98° 3.59 mm	127° 2.56 mm	67.62° 2.08 mm
78.07° 2.18 mm	189.49° 3.15 mm	106.19° 2.39 mm	245.23° 3.42 mm	188.58° 3.14 mm	352.92° 3.74 mm	319.94° 3.68 mm
179.39° 3.2 mm	222.99° 3.33 mm	224.62° 3.34 mm	276.98° 3.54 mm	304.49° 3.63 mm	21.5° 1.39 mm	72.16° 2.12 mm

## 5. Conclusion

The paper introduces a single transmitarray antenna structure with dual-focus using the chess-board arrangement. The dual-focus of the transmitarray in near-field and a dual-beam directions in the far-field are designed. The transmitarray consists of 13×13 unit-cell elements made of a perforated dielectric sheet. Different transmitarrays with dual-focus in the NF/NF, FF/FF, NF/FF and FF/NF regions are designed using the chess-board arrangement. The FF/NF-focused transmitarray introduces a maximum gains of 23.45 dB/17.26 dB with a side lobe level of -15.7 dB/-8 dB in the E-/H-plane. In the same structure the array produced power density closer to each other with -10 dB spot area of 63×60 mm<sup>2</sup> at a distance R<sub>o</sub> = 310 mm. The NF/NF transmitarray with power focused in two near field distances at R<sub>o1</sub>=310 mm and R<sub>o2</sub>=347 mm is designed. Finally, dual-beam transmitarray is proposed to obtain two beams in different directions with angles 20° and -20° in the same structure using the chess-board arrangement. The maximum gains for beam at θ = 20° is 15 dB and for the beam at θ = -20° is 17 dB.

## References

[1] O. Yurduseven , Compact parabolic reflector antenna design with cosecant-squared radiation pattern, *Microwaves, Radar and Remote Sensing Symposium, Kiev, Ukraine*, pp. 382-385, August 2011.

[2] G. M. Rebeiz, K. J. Koh, Tiku Yu, D. Kang, C. Y. Kim, Y. Atesal, B. Cetinoneri, S. Y. Kim, and D. Shin, Highly dense microwave and millimeter wave phased array T/R modules and butler matrices using CMOS and SiGe RFICs, *IEEE International Symposium on, Phased Array Systems and Technology (ARRAY), Boston, Massachusetts, USA*, pp. 245-249, October 2010.

[3] M. Ruphuy, Z. Ren, and O. M. Ramahi, Flat far field lenses and reflectors, *Progress In Electromagnetics Research M, (PIER M)*, vol.34, pp.163-170, 2014.

[4] J. Huang and J. A. Encinar, *Reflectarray Antennas, IEEE Press, John Wiley and Sons, New Jersey, USA*, 2008.

[5] S. H. Zainud-Deen, W. M. Hassen, and H. A. Malhat, Investigation into the effect of solar cells on the DRA reflectarray/transmitarray antenna design, *32<sup>nd</sup> National Radio Science Conference (NRSC), 6<sup>th</sup> of October City, Egypt*, pp. 1-8, March 2015.

[6] S. H. Zainud-Deen, S. M. Gaber, H. A. Malhat, and K. H. Awadalla, Perforated transmitarray-enhanced circularly polarized antenna for high-gain multi-beam radiation, *International Symposium on Antennas and Propagation (ISAP 2013), Nanjing, China*, pp. 484-487, October 2013.

[7] M. K. Al-Nuaimi and W. Hong, Discrete dielectric reflectarray and lens for E-band with different feed, *IEEE Antennas and Wireless Propagat. Letters*, vol.13, pp. 947-950, March 2014.



- [8] S. H. Zainud-Deen, N. El-Shalaby, S. M. Gaber, H. A. Malhat, and K. H. Awadalla, Reflectarrays mounted on or embedded in cylindrical or spherical surfaces, *Middle East Conference on Antennas and Propagat. (MECAP 2012)*, Cairo, Egypt, pp.1-6, December 2012.
- [9] L. Dussopt, H. Kaouach, J. Lanteri, and R. Sauleau, Circularly-polarized discrete lens antennas in 60-GHz band, *Radio engineering*, vol. 20, no.4, pp. 733-738, December 2011.
- [10] S. M. Gaber, Analysis and Design of Reflectarrays/Transmitarrays Antennas, *Ph.D Thesis, Faculty of Electronic Engineering, Minoufia University, Menouf, Egypt*, 2013.
- [11] S. H. Zainud-Deen, W. M. Hassen, H. A. Malhat, and K. H. Awadalla, Radiation characteristics enhancement of dielectric resonator antenna using solid/discrete dielectric lens, *Advanced Electromagnetics*, vol. 4, no. 1, February 2015.
- [12] J. Y. Lau and S. V. Hum, A wideband reconfigurable transmitarray element, *IEEE Trans. Antennas Propagat.*, vol. 60, no. 3, pp. 1303-1311, March 2012.
- [13] E. Eridl, K. Topalli, O. Zorlu, T. Toral, E. Yildirim, H. Kulah, and O. A. Civi, A reconfigurable microfluidic transmitarray unit cell, *7<sup>th</sup> European Conference on Antennas and Propagat. (EUCAP)*, Gothenburg, Sweden, pp. 2957-2960, April 2013.
- [14] A. H. Abdelrahman, P. Nayeri, A. Z. Elsherbeni, and F. Yang, Analysis and design of wideband transmitarray antennas with different unit-cell phase ranges, *IEEE Antennas and propagat. Society International Symposium (APSURSI)*, Memphis, USA, pp. 1266-1267, July 2014.
- [15] J. Venter, M. Pelouskova, Outcomes and complications of a multifocal toric intraocular lens with a surface-embedded near section, *Journal of Contaract & Refractive Surgery*, vol. 39, pp. 859-866, June 2013.
- [16] R. Siragusa, P. Lemaître-Auger, and S. Tedjini, Tunable near-field focused circular phase-array antenna for 5.8-GHz RFID applications, *IEEE Antennas and Wireless Propagat. Letters*, vol. 10, pp. 33-36, March 2011.
- [17] A. Buffi, P. Nepa, and G. Manara, Design criteria for near-field-focused planar arrays, *IEEE Antennas Propag. Mag.*, vol. 54, no. 1, pp. 40-50, February 2012.
- [18] F. Tofigh, J. Nourinia, M. N. Azarmanesh, and K. M. Khazaei, Near-field focused array microstrip planar antenna for medical applications, *IEEE Antennas and Wireless Propagat. Letters*, vol. 13, pp. 951-954, May 2014.
- [19] K. D. Stephan, J. B. Mead, D. M. Pozar, L. Wang, and J. A. Pearce, A near field focused microstrip array for a radiometric temperature sensor, *IEEE Trans. Antennas Propagat.*, vol. 55, no. 4, pp. 1199-1203, April 2007.
- [20] A. Buffi, A. Serra, P. Nepa, G. Manara, and M. Luise, Near field focused microstrip arrays for gate access control systems, *In Proc. IEEE Antennas Propag. Symp.*, Charleston, SC, USA, pp. 1-4, June 2009.
- [21] M. Bogosanovic and A. G. Williamson, Microstrip antenna array with a beam focused in the near-field zone for application in noncontact microwave industrial inspection, *IEEE Trans. Instrum. Meas.*, vol. 56, no. 6, pp. 2186-2195, December 2007.
- [22] B. Shrestha, A. Elsherbeni, and L. Ukkonen, UHF RFID reader antenna for near-field and far-field operations, *IEEE Antenna and Wireless Propag.*, vol. 10, pp. 1274-1277, November 2011.
- [23] R. Siragusa, P. Lemaître-Auger, and S. Tedjini, Near field focusing circular microstrip antenna array for RFID applications, *In Proc. IEEE APSURSI, Charleston, SC*, pp. 1-4, June 2009.
- [24] S. H. Zainud-Deen, H. A. Malhat, K. H. Awadalla, 8×8 near-field focused circularly polarized cylindrical DRA array for RFID applications, *The applied computational Electromagnetics (ACES)*, vol. 27, no. 1, pp. 42-48, 2012.
- [25] User's manual of CST Microwave Studio 2012.
- [26] S. H. Zainud-Deen, S. M. Gaber, H. A. Malhat, and K. H. Awadalla, Cylindrical perforated transmitarrays, *2<sup>nd</sup> Middle East Conf. on Antenna and Proagat. (MECAP)*, Egypt, pp. 1-7, December 2013.
- [27] R. C. Hansen, Focal region characteristics of focused array antennas, *IEEE Trans. Antennas Propagat.*, vol. 33, no. 12, 1328-1337, December 1985.



**Saber Helmy Zainud-Deen:** was born in Menouf, Egypt, on November 15, 1955. He received the B.Sc and M.Sc degrees from Menoufia University in 1973 and 1982 respectively, and the Ph.D degree in antenna engineering from Menoufia University, Egypt in 1988. He is currently a professor in the

department of electrical and electronic engineering in the faculty of electronic engineering, Menoufia University, Egypt. His research interest at present include microstrip and leaky wave antennas, DRA, RFID, optimization techniques, FDFD and FDTD, scattering problems and breast cancer detection.



**W. M. Hassan:** was born in Shebien El-Kom, Menoufia, Egypt, on January 11, 1981. She received the B. Sc M. Sc degrees from Menoufia University in 2002 and 2010. She is currently assistant researcher in electronics research institute (ERI). Her research interest at FDFD, Scattering, breast cancer detection, chiral materials,

metamaterials, DRA, transmitarray, reflectarray, solar cell, and graphene.



**Hend Abd El-Azem Malhat:** was born in Menouf, Egypt, on December 12, 1982. She received the B. Sc and M. Sc degrees from Menoufia University in 2004 and 2007 respectively. She received her Ph.D degree in Antenna Engineering from Menoufia University, Egypt 2011. She is currently an associated professor in the department of electrical and electronic engineering in the faculty of electronic engineering, Menoufia University, Egypt. Her research interest at present include Graphene antennas, plasma antennas, wavelets technique, transmitarray, reflectarray and RFID.